Int. J. Heat Mass Transfer. Vol. 33. No. 3, pp. 517–528. 1990
Printed in Great Britain

0017–9310/90 $3.00 + 0.00
Pergamon Press plc

The effects of heat conduction in the wall on the development of recirculating combined convection flows in vertical tubes

P. J. HEGGS
Department of Chemical Engineering, University of Bradford, Bradford BD7 1DP, U.K.

and

D. B. INGHAM and D. J. KEEN
Department of Applied Mathematical Studies, University of Leeds, Leeds LS2 9JT, U.K.

(*Received* 10 *January* 1989 *and in final form* 19 *April* 1989)

Abstract—The effects of wall heat conduction on a steady laminar combined convection water flow in a vertical pipe are investigated numerically. The Prandtl, Reynolds and Grashof numbers of the flow are fixed at 7.0, 50 and −10000, respectively, and reverse flow is present in most of the flows considered. Investigations are carried out as the wall to fluid conductivity ratio and the ratio of the outside to the inside radii of the pipe wall are allowed to vary. Comparisons with a flow in which no wall solution domain is considered show that very significant changes in the flow and temperature distributions may be observed when a wall domain is taken into account.

1. INTRODUCTION

IN MANY theoretical studies of convection flows in vertical ducts the conduction of heat in the wall of the duct is overlooked. In practice, especially when large temperature gradients are present, the temperature and temperature gradient at the inside of the duct wall are dependent not only on the thermal properties of the fluid and the characteristics of the flow, but also on the thermal conduction in the duct wall. Thus, in modelling many physical situations, it is desirable to consider a thermal problem in both the fluid and wall domains, as well as the momentum problem in the fluid.

A review of laminar convection in ducts of various cross-sections is presented by Shah and London [1] and brief references are made to conjugate problems which allow for conductance in the wall of the duct. In recent years more attention has been paid to the importance of the interaction of the heat transfer mechanisms in the wall and fluid domains and good examples of this can be found in the investigations of Barozzi and Pagliarini [2–4], Mori *et al.* [5, 6], Zariffeh *et al.* [7], Faghri and Sparrow [8] and Campo and Rangel [9]. Barozzi and Pagliarini assume a fully developed velocity profile in the fluid domain and avoid solving the thermal problem in the fluid domain by solving the energy equation in the wall using finite elements in an iterative procedure which involves the updating of the interfacial temperature after each iteration. The wall solution region in these investigations is restricted to the heat transfer section so that no account is taken of upstream and downstream heat conduction prior to and after the heat transfer region. This is also true of the work of Mori *et al.*, where fully developed flow profiles are also assumed in cylindrical and parallel plate geometries, respectively. Here the problem is solved by assuming the interfacial temperature to be in the form of a power series and finding the unknown coefficients by solving the energy equations in the solid and fluid and equating the temperature and heat fluxes at the interface. Zariffeh *et al.* and Faghri and Sparrow use a different approach which again involves the assumption of fully developed flow in the fluid. They both assume a thin wall, so the wall solution domain can be replaced by a suitable boundary condition at the extreme of the fluid domain and the elliptic energy equation in the fluid is solved using iterative techniques. Campo and Rangel make the assumptions of negligible temperature gradients in the wall and fluid domains and let the velocity profile in the fluid be represented by its mean value, and thus are able to solve the resulting ordinary differential equations using an analytic approach. The problem with the above investigations is the number of assumptions that are made in order to simplify the governing equations. In particular no attention is paid to the possible change of the velocity profile of the fluid due to the free convection effects, which must certainly be present in many industrial applications where large temperature gradients are often involved.

Many investigations have been carried out into combined convection flows in which no account is

NOMENCLATURE

a radius of the inside of the duct wall
a^* radius of the outside of the duct wall
A_s coefficient of $X^s \sin s\lambda$ in the expression for θ_w near $Z = b/(a\,Re)$, $R = a^*/a$
b axial location of the beginning of the heated region
B_1, B_2 constants in the expression for θ_w near $Z = b/(a\,Re)$, $R = a^*/a$
C transformation parameter
d position at which the scaling in the axial direction is introduced
f friction factor
$f(\lambda)$ particular integral of equation (29)
g acceleration due to gravity
$g(\lambda)$ part of the complimentary function of equation (29)
Gr Grashof number, $g\beta(T_e - T_\infty)a^3/\nu^2$
G^z finite difference grid for $0 \leqslant Z \leqslant d$, $0 \leqslant R \leqslant 1$
G^{zw} finite difference grid for $0 \leqslant Z \leqslant d$, $1 < R \leqslant a^*/a$
G^ξ finite difference grid for $d \leqslant Z < \infty$, $0 \leqslant R \leqslant 1$
$G^{\xi w}$ finite difference grid for $d \leqslant Z < \infty$, $1 < R \leqslant a^*/a$
h local heat transfer coefficient
k thermal conductivity of the fluid
K_r wall to fluid conductivity ratio
N number of finite difference steps across the duct
NN number of finite difference steps along the duct
N^w number of finite difference steps across the wall
N^ξ number of finite difference steps in the Z-direction on G^ξ
Nu local Nusselt number, ha/k
p pressure
P dimensionless pressure, $p/\rho_0 u_m^2 - gz[b(T_\infty - T_e) - 1]/u_m^2$
Pe Péclet number, $Re\,Pr$
Pr Prandtl number, ν/α
r radial coordinate
R dimensionless radial coordinate, r/a
Re Reynolds number, au_m/ν
s power of W in the complimentary function of equation (29)
T temperature
u axial velocity
U dimensionless axial velocity, u/u_m
v radial velocity
V dimensionless radial velocity, v/u_m
X local coordinate in the wall near $Z = b/(a\,Re)$, $R = a^*/a$
z axial coordinate
Z dimensionless axial coordinate, $z/(a\,Re)$.

Greek symbols

α molecular thermal diffusivity
β coefficient of thermal expansion, $(-1/\rho)(\partial\rho/\partial T_f)$
θ dimensionless temperature, $\theta_{f,w} = (T_{f,w} - T_\infty)/(T_e - T_\infty)$
$\theta_1, \theta_2, \theta_3$ three finite difference values of θ_w immediately upstream of $Z = b/(a\,Re)$, $R = a^*/a$
κ dimensional axial finite difference step on G^{zw}
λ local coordinate in the wall near $Z = b/(a\,Re)$, $R = a^*/a$
μ dynamic viscosity of the fluid
ν kinematic viscosity of the fluid
ξ dimensionless axial coordinate on G^ξ, $1 - 1/(1 + C(Z - d))$
ρ variable density of the fluid
ρ_o density of the fluid at $T_f = T_\infty$
ψ dimensionless stream function
Ω dimensionless vorticity.

Subscripts

e entry value
f value within the fluid
m flow average value
NN value at the NNth axial location
w value within the wall
∞ fully developed value and the boundary temperature value over the final section of the duct wall.

taken of heat conduction in the wall, and three good examples of these in which the axial diffusion terms in the fluid are retained in the governing equations are in the papers of Zeldin and Schmidt [10], Chow *et al.* [11] and Morton *et al.* [12]. In these investigations, wall temperature or heat flux boundary conditions are applied at the extreme of the fluid domain. The governing elliptic equations are then non-dimensionalized, expressed in finite difference form and solved using relaxation techniques. In the studies of Chow *et al.* and Morton *et al.* situations are considered where the duct walls are heated over finite sections and in the investigation of Morton *et al.* situations are considered where flow reversals are present at one or more places in the flow.

The governing parameters in the conjugate heat transfer problems mentioned above are, the Péclet number of the fluid, Pe, the ratio of the radii of the outside and the inside of the pipe wall, a^*/a, the wall to fluid conductivity ratio, K_r, and, where relevant,

the non-dimensional length of the heating or cooling sections. The governing parameters in the developing flow situations listed above are, the Reynolds number, Re, the Prandtl number, Pr, the Grashof number, Gr, and, where relevant, the length of the heating or cooling sections.

In the present investigation, the work of Morton *et al.* [12] is extended and a solution is obtained to a conjugate heat transfer situation by solving the governing equations in the solid and fluid phases simultaneously, by means of finite difference techniques and a relaxation procedure. Several realistic values of the ratio a^*/a are considered for values of K_r relevant to various typical wall materials and with water as the fluid in the duct. The Reynolds and Grashof numbers of the flow are fixed for all the investigations so that comparisons can easily be made, and Gr is chosen to be large so that in most of the situations considered flow reversals are present in the fluid.

The results are presented in terms of stream function and temperature contours around the thermal entrance of the duct and also in terms of plots of flow average temperature, local Nusselt number and friction factor times Reynolds number against axial distance. The results illustrate the fact that by changing the conductivity and thickness of a pipe wall the characteristics of the flow and the heat transfer may be drastically affected.

2. THE MODEL AND GOVERNING EQUATIONS

The model consists of steady laminar combined convection of a fluid with velocity, (v, u), and temperature, T_f, in the semi-infinite domain $0 \leqslant r \leqslant a$, $0 \leqslant z < \infty$ which is bounded by a wall contained in the domain $a \leqslant r \leqslant a^*$, $0 \leqslant z < \infty$ where the temperature is given by T_w, as illustrated in Fig. 1. Thermal boundary conditions are applied at $r = a^*$, so that the temperature at $r = a$, which is dependent upon the properties of both the fluid and the wall, is able to attain a distribution which is appropriate to a real physical situation. As a comparison, situations are also considered where the temperature boundary conditions are applied at $r = a$, and no wall solution domain is considered. However, the following analysis concentrates on the more complicated situation where the wall domain is included in the problem. Fluid at constant temperature, T_e, is assumed to flow into the duct at $z = 0$ with a fully developed parabolic velocity profile, $(0, u_e)$, and the fluid is heated over $z > b$ where b is chosen to be large enough so that the boundary condition at $z = 0$ is a good approximation to $z = -\infty$ where the flow is fully developed and isothermal. Over the heated section of the tube, $z > b$, the temperature of the outside of the tube wall is maintained constant at T_∞, whilst over the preceding, 'entry', section, $0 \leqslant z < b$, a zero heat flux boundary condition is applied at the outside of the wall.

The acceleration due to gravity, g, acts vertically downwards, in the opposite direction to the forced convection. The fluid is considered to be Newtonian with constant dynamic viscosity, thermal conductivity, specific heat capacity and coefficient of expansion. The wall is considered to have a constant thermal conductivity. Density variations are neglected everywhere except in the buoyancy term of the vertical momentum equation (Boussinesq approximation). These assumptions are made in order to keep the

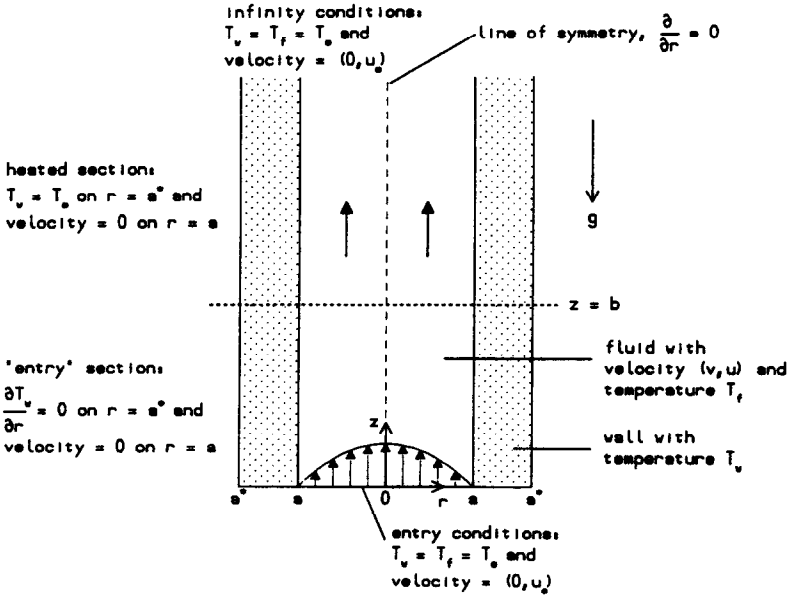

FIG. 1. Schematic view of the mathematical model and the wall and fluid solution domains for the cylindrical duct.

model as simple as possible, although inclusion of variations in some of the physical properties should not in theory be difficult to introduce into the numerical analysis. Viscous dissipation in the fluid is ignored as it was shown to have only a small effect by Collins [13].

The governing equations are the continuity, axial momentum, radial momentum, and energy equations in the fluid and the energy equation in the wall, and these can be written, respectively, in the following form [14]:

$$\frac{\partial u}{\partial z}+\frac{\partial v}{\partial r}+\frac{v}{r}=0 \tag{1}$$

$$u\frac{\partial u}{\partial z}+v\frac{\partial u}{\partial r}=-\frac{1}{\rho}\frac{\partial p}{\partial z}+\nu\left[\frac{\partial^2 u}{\partial z^2}+\frac{1}{r}\frac{\partial}{\partial r}\left(r\frac{\partial u}{\partial r}\right)\right]-g \tag{2}$$

$$u\frac{\partial v}{\partial z}+v\frac{\partial v}{\partial r}=-\frac{1}{\rho}\frac{\partial p}{\partial r}+\nu\left[\frac{\partial^2 v}{\partial z^2}+\frac{1}{r}\frac{\partial}{\partial r}\left(r\frac{\partial v}{\partial r}\right)-\frac{v}{r^2}\right] \tag{3}$$

$$u\frac{\partial T_f}{\partial z}+v\frac{\partial T_f}{\partial r}=\alpha\left[\frac{\partial^2 T_f}{\partial z^2}+\frac{1}{r}\frac{\partial}{\partial r}\left(r\frac{\partial T_f}{\partial r}\right)\right] \tag{4}$$

$$0=\frac{\partial^2 T_w}{\partial z^2}+\frac{1}{r}\frac{\partial}{\partial r}\left(r\frac{\partial T_w}{\partial r}\right) \tag{5}$$

where α is the molecular thermal diffusivity, ν the kinematic viscosity, ρ the density and p the pressure of the fluid. Equation (5) assumes a steady state and zero heat generation within the wall. The boundary conditions for the problem are as follows:

$$\text{at } r=0,\quad 0\leqslant z<\infty:\quad v=0,\quad \frac{\partial u}{\partial r}=0,\quad \frac{\partial T_f}{\partial r}=0 \tag{6}$$

$$\text{at } r=a,\quad 0\leqslant z<\infty:\quad v=0,\quad u=0,\quad T_w=T_f,\quad k_w\frac{\partial T_w}{\partial r}=k_f\frac{\partial T_f}{\partial r} \tag{7}$$

$$\left.\begin{aligned}&\text{at } r=a^*,\quad 0\leqslant z<b:\quad \frac{\partial T_w}{\partial r}=0\\ &\qquad\qquad b\leqslant z<\infty:\quad T_w=T_\infty\end{aligned}\right\} \tag{8}$$

$$\left.\begin{aligned}&\text{at } z=0,\\ &\quad 0\leqslant r\leqslant a:\quad v=0,\quad u=u_e,\quad T_f=T_e\\ &\quad a<r\leqslant a^*:\quad \frac{\partial T_w}{\partial z}=0\end{aligned}\right\} \tag{9}$$

$$\left.\begin{aligned}&\text{at } z\to\infty,\\ &\quad 0\leqslant r\leqslant a:\quad v=0,\quad u=u_\infty,\quad T_f=T_\infty\\ &\quad a<r\leqslant a^*:\quad \frac{\partial T_w}{\partial z}=0.\end{aligned}\right\} \tag{10}$$

The velocities $u_e=u_\infty$ correspond to parabolic velocity profiles and k_f and k_w are the thermal conductivities of the fluid and wall, respectively.

The Boussinesq approximation involves replacing ρ by $\rho_o[1-\beta(T_f-T_e)]$ in the buoyancy term of equation (2) and by ρ_o elsewhere. Here ρ_o is the density of the fluid at $T_f=T_e$ and $\beta=(-1/\rho)(\partial\rho/\partial T_f)$ is the coefficient of expansion with respect to T_f. Now simplify equations (1)–(5) using the following non-dimensionalization:

$$\left.\begin{aligned}&v=u_m V,\quad u=u_m U,\quad r=aR,\quad z=a\,Re\,Z\\ &p=g\rho_o z[\beta(T_\infty-T_e)-1]+\rho_o u_m^2 P,\\ &T_{f,w}=T_\infty+(T_e-T_\infty)\theta_{f,w}\end{aligned}\right\} \tag{11}$$

where u_m is a characteristic velocity taken in this study to be the flow average velocity and $Re=au_m/\nu$ is the Reynolds number of the flow. Defining the stream function, ψ, to satisfy the continuity equation (1) and introducing the vorticity, Ω, as follows:

$$V=\frac{1}{Re}\frac{1}{R}\frac{\partial\psi}{\partial Z},\quad U=-\frac{1}{R}\frac{\partial\psi}{\partial R} \tag{12}$$

$$\Omega=\frac{1}{Re}\frac{\partial V}{\partial Z}-\frac{\partial U}{\partial R} \tag{13}$$

and eliminating the pressure between equations (2) and (3), equations (1)–(5) reduce to the following non-dimensional form:

$$\Omega R=\frac{1}{Re^2}\frac{\partial^2\psi}{\partial Z^2}+\frac{\partial^2\psi}{\partial R^2}-\frac{1}{R}\frac{\partial\psi}{\partial R} \tag{14}$$

$$\frac{1}{R}\frac{\partial\psi}{\partial Z}\frac{\partial\Omega}{\partial R}-\frac{1}{R}\frac{\partial\psi}{\partial R}\frac{\partial\Omega}{\partial Z}-\frac{\Omega}{R^2}\frac{\partial\psi}{\partial Z}=\frac{1}{Re^2}\frac{\partial^2\Omega}{\partial R^2}+\frac{\partial^2\Omega}{\partial R^2}+\frac{1}{R}\frac{\partial\Omega}{\partial R}-\frac{\Omega}{R^2}-\frac{Gr}{Re}\frac{\partial\theta_f}{\partial R} \tag{15}$$

$$\frac{1}{R}\frac{\partial\psi}{\partial Z}\frac{\partial\theta_f}{\partial R}-\frac{1}{R}\frac{\partial\psi}{\partial R}\frac{\partial\theta_f}{\partial Z}=\frac{1}{Pr}\left\{\frac{1}{Re^2}\frac{\partial^2\theta_f}{\partial Z^2}+\frac{\partial^2\theta_f}{\partial R^2}+\frac{1}{R}\frac{\partial\theta_f}{\partial R}\right\} \tag{16}$$

$$0=\frac{1}{Re^2}\frac{\partial^2\theta_w}{\partial Z^2}+\frac{\partial^2\theta_w}{\partial R^2}+\frac{1}{R}\frac{\partial\theta_w}{\partial R} \tag{17}$$

where $Gr=g\beta(T_e-T_\infty)a^3/\nu^2$ is the Grashof number and $Pr=\nu/\alpha$ the Prandtl number. Boundary conditions (6)–(10) become:

$$\text{at } R=0,\quad 0\leqslant Z<\infty:\quad \psi=\tfrac{1}{2},\quad \Omega=0,\quad \frac{\partial\theta_f}{\partial R}=0 \tag{18}$$

$$\text{at } R=1,\quad 0\leqslant Z<\infty:\quad \psi=0,\quad \frac{\partial\psi}{\partial R}=0$$

$$\theta_w=\theta_f,\quad K_r\frac{\partial\theta_w}{\partial R}=\frac{\partial\theta_f}{\partial R} \tag{19}$$

$$\left.\begin{aligned} &\text{at } R = a^*/a, \quad 0 \leqslant Z < b/(a\,Re): \quad \frac{\partial \theta_f}{\partial R} = 0 \\ &\qquad\qquad\qquad\quad b/(a\,Re) \leqslant Z < \infty: \quad \theta_w = 0 \end{aligned}\right\} \tag{20}$$

$$\left.\begin{aligned} &\text{at } Z = 0, \\ &0 \leqslant R \leqslant 1: \quad \psi = \tfrac{1}{2}(1-R^2)^2, \quad \Omega = 4R, \quad \theta_f = 1 \\ &1 < R \leqslant a^*/a: \quad \frac{\partial \theta_w}{\partial Z} = 0 \end{aligned}\right\} \tag{21}$$

$$\left.\begin{aligned} &\text{as } Z \to \infty, \\ &0 \leqslant R \leqslant 1: \quad \psi = \tfrac{1}{2}(1-R^2)^2, \quad \Omega = 4R, \quad \theta_f = 0 \\ &1 < R \leqslant a^*/a: \quad \frac{\partial \theta_w}{\partial Z} = 0 \end{aligned}\right\} \tag{22}$$

where $K_r = k_f/k_w$ is the fluid to wall conductivity ratio.

The elliptic equations (14)–(17) give the desired description of the problem under consideration and they must be solved subject to boundary conditions (18)–(22). The governing parameters in the problem are thus the Reynolds number, Re, the Prandtl number, Pr, the ratio of the Grashof to the Reynolds number, Gr/Re, the fluid to wall conductivity ratio, K_r, and the ratio of the radii of the outside and the inside of the tube wall, a^*/a.

3. THE SOLUTION TECHNIQUE

In order to satisfy boundary conditions (22) when solving the above problem a scaling is used in the axial direction. This scaling, as used in Keen [14], Morton *et al.* [12] and Zeldin and Schmidt [10], is applied over the region $d < Z < \infty$ and is defined as

$$\xi = 1 - 1/(1 + C(Z-d)) \quad \text{or} \quad Z = (\xi/C)/(1-\xi) + d \tag{23}$$

where ξ is a new axial variable which lies in the range $0 \leqslant \xi \leqslant 1$, C is a transformation parameter to be defined later and $Z = d$ is a station far enough downstream from $Z = b/(a\,Re)$ for the differences caused by the wall to be negligible. Equations (14)–(17) under this transformation become

$$\Omega R = \frac{1}{Re^2}\left[\frac{\partial^2 \psi}{\partial \xi^2}\left(\frac{d\xi}{dZ}\right)^2 + \frac{\partial \psi}{\partial \xi}\frac{d^2\xi}{dZ^2}\right] + \frac{\partial^2 \psi}{\partial R^2} - \frac{1}{R}\frac{\partial \psi}{\partial R} \tag{24}$$

$$\frac{1}{R}\frac{d\xi}{dZ}\left[\frac{\partial \psi}{\partial \xi}\frac{\partial \Omega}{\partial R} - \frac{\partial \psi}{\partial R}\frac{\partial \Omega}{\partial \xi} - \frac{\Omega}{R}\frac{\partial \psi}{\partial \xi}\right] = \frac{1}{Re^2}\left[\frac{\partial^2 \Omega}{\partial \xi^2}\left(\frac{d\xi}{dZ}\right)^2 + \frac{\partial \Omega}{\partial \xi}\frac{d^2\xi}{dZ^2}\right] + \frac{\partial^2 \Omega}{\partial R^2} + \frac{1}{R}\frac{\partial \Omega}{\partial R} - \frac{\Omega}{R^2} - \frac{Gr}{Re}\frac{\partial \theta_f}{\partial R} \tag{25}$$

$$\frac{1}{R}\frac{d\xi}{dZ}\left[\frac{\partial \psi}{\partial \xi}\frac{\partial \theta_f}{\partial R} - \frac{\partial \psi}{\partial R}\frac{\partial \theta_f}{\partial \xi}\right] = \frac{1}{Pr}\left\{\frac{1}{Re^2}\left[\frac{\partial^2 \theta_f}{\partial \xi^2}\left(\frac{d\xi}{dZ}\right)^2 + \frac{\partial \theta_f}{\partial \xi}\frac{d^2\xi}{dZ^2}\right] + \frac{\partial^2 \theta_f}{\partial R^2} + \frac{1}{R}\frac{\partial \theta_f}{\partial R}\right\} \tag{26}$$

$$0 = \frac{1}{Re^2}\left[\frac{\partial^2 \theta_w}{\partial \xi^2}\left(\frac{d\xi}{dZ}\right)^2 + \frac{\partial \theta_w}{\partial \xi}\frac{d^2\xi}{dZ^2}\right] + \frac{\partial^2 \theta_w}{\partial R^2} + \frac{1}{R}\frac{\partial \theta_w}{\partial R}. \tag{27}$$

The problem can now be split into four solution domains, these being $0 \leqslant Z \leqslant d$, $0 \leqslant R \leqslant 1$ where equations (14)–(16) and boundary conditions (18), (19) and (21) for ψ, Ω and θ_f apply, $d < Z < \infty$, $0 \leqslant R \leqslant 1$ where equations (24)–(26) and boundary conditions (18), (19) and (22) for ψ, Ω and θ_f hold, $0 \leqslant Z \leqslant d$, $1 < R \leqslant a^*/a$ where equation (17) and boundary conditions (19)–(21) for θ_w apply and $d < Z < \infty$, $1 < R \leqslant a^*/a$ where equation (27) and boundary conditions (19), (20) and (22) for θ_w hold. To solve the problem these equations and boundary conditions are expressed in finite difference form on the four regular grids G^z, G^ξ, G^{zw} and $G^{\xi w}$, where G^z covers the domain $0 \leqslant Z \leqslant d$, $0 \leqslant R \leqslant 1$ and consists of $N+1$ points in the radial direction and $NN+1$ points in the axial direction, G^ξ covers the domain $d < Z < \infty$, $0 \leqslant R \leqslant 1$ and consists of $N+1$ points in the radial direction and $N^\xi+1$ points in the ξ-direction, G^{zw} covers the domain $0 \leqslant Z \leqslant d$, $1 < R \leqslant a^*/a$ and consists of N^w+1 points in the radial direction and $NN+1$ points in the axial direction and $G^{\xi w}$ covers the domain $d < Z < \infty$, $1 < R \leqslant a^*/a$ and consists of N^w+1 points in the radial direction and $N^\xi+1$ points in the ξ-direction. The solutions on these two grids are matched up at $Z = d$ and the value of the parameter C is chosen so that the step size between the axial locations Z_{NN+2} and $Z_{NN+1} = d$ is the same as the distance between axial locations Z_{NN+1} and Z_{NN}. This leads to [12]

$$C = 1/((N^\xi - 1)K) \tag{28}$$

where $K = d/NN$ is the finite difference step size in the axial direction on G^z and G^{zw}.

Central differences are used in the radial direction for both first and second derivatives, however attempts to do the same in the axial direction produce oscillations in the solution. These oscillations are overcome by using either backward or forward differencing in the axial first derivative terms in the fluid, depending upon whether the flow at a particular point is in the same or the opposite direction to the forced convection, respectively. The vorticity of the fluid at the inside of the duct wall is determined to second-order accuracy using Taylor series expansions of ψ and Ω at $R = 1$, the fact that $\partial\psi/\partial R = 0$ at $R = 1$,

and equations (14) and (24) evaluated at $R = 1$. The temperature at the centerline is given to second-order accuracy using $\partial\theta/\partial R = 0$ at $R = 0$ and equations (16) and (26) evaluated at $R = 0$. The derivative thermal boundary condition at $R = 1$ is dealt with by using first-order differencing on each side of $R = 1$, the continuity boundary condition at $R = 1$ is automatically satisfied by using the last point in the fluid as the first point in the wall and the zero heat flux boundary condition at $R = a^*/a$ for $0 < Z < b/(a\,Re)$ is satisfied by using first-order backward differencing. The solution to the problem is obtained iteratively by sweeping across the grids G^z, G^{zw}, G^ξ and $G^{\xi w}$ from $Z = 0$ to $\xi = 1$, relaxing the relevant finite difference equations at each point on the four grids. In the calculations the finite difference equations for Ω and θ_f must be underrelaxed, those for θ_f more so than those for Ω, however, a relaxation parameter of unity is used for the finite difference equations involving ψ and the finite difference equations for θ_w are overrelaxed. Problems, in terms of accuracy and convergence, can occur at $R = a^*/a$ for the finite difference variable θ_w, just upstream of $Z = b/(a\,Re)$, due to the discontinuity in temperature gradient at this point. This is also found to cause convergence problems for the variable Ω on the inside of the duct wall in the vicinity of $Z = b/(a\,Re)$. The inaccuracies are overcome in the following manner. Consider a new coordinate system, (X, λ), inside the wall as shown in Fig. 2. In terms of the new coordinates equation (17) becomes

$$0 = \frac{\partial^2\theta_w}{\partial X^2} + \frac{1}{X}\frac{\partial\theta_w}{\partial X} + \frac{1}{X^2}\frac{\partial^2\theta_w}{\partial\lambda^2}. \tag{29}$$

The particular integral, $\theta_w = f(\lambda)$, of equation (29) must be $f = 0$ in order to satisfy the two boundary conditions $\theta_w = 0$ for $\lambda = 0$ and $\partial\theta_w/\partial\lambda = 0$ for $\lambda = \pi$. To find the complimentary function put $\theta_w = X^s g(\lambda)$, which leads to

$$\theta_w = \sum_s A_s X^s \sin s\lambda \tag{30}$$

where $s = 1/2, 3/2, \ldots$ and the coefficients A_s are to be determined from the boundary conditions. Hence to $O(X^2)$

$$\theta_w = B_1 X^{1/2}\sin\lambda/2 + B_2 X^{3/2}\sin 3\lambda/2 \tag{31}$$

where $B_1 = A_{1/2}$ and $B_2 = A_{3/2}$. Putting $\lambda = \pi$, the finite difference value of θ_w immediately upstream of $Z = b/(a\,Re)$ can be expressed as

$$\theta_1 = B_1\kappa^{1/2} - B_2\kappa^{3/2} \tag{32}$$

where κ is the dimensional axial finite difference step on G^{zw}. Now B_1 and B_2 can be determined using the two finite difference values for θ_w immediately upstream of θ_1 to give

$$\theta_1 = 2^{1/2}\theta_2 - 3^{-1/2}\theta_3 \tag{33}$$

where θ_2 and θ_3 are as indicated in Fig. 2. Equation (33) gives an accurate value for θ_1 so long as $\kappa \ll 1$, since this implies that $X \ll 1$.

Despite the above refinements, problems with very slow convergence are encountered upstream of $Z = b/(a\,Re)$ when K_r becomes large ($\gg 100$). This is due to the fact that the 'entry' region between $Z = 0$ and $b/(a\,Re)$ is not long enough to allow the heat in the wall to conduct as far upstream as it would like. The thermal wall boundary condition (21) will therefore be isolated causing inaccuracies and slow convergence. These problems could be overcome by introducing a second scaled region going upstream to $Z = -\infty$, this, however, is beyond the scope of this investigation. For the above reasons the investigations in this study are restricted to situations for which $K_r \leqslant 50$ where accurate solutions can be obtained.

Convergence is assumed to have occurred when the average change in the finite difference variables between consecutive iterations has fallen below 10^{-8}. This value is smaller than would normally be required because of the slow convergence of the variable Ω for the reasons discussed above. When the average change in all of the finite difference variables falls below 10^{-8},

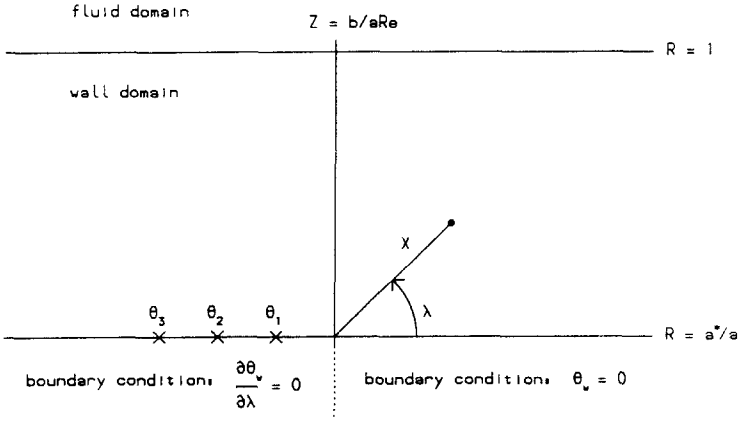

FIG. 2. Schematic view of the (X, λ) coordinate system within the wall in the vicinity of $Z = b/(a\,Re)$ and $R = a^*/a$.

the maximum change in the variable Ω is generally just below 10^{-6}. For some situations convergence may be achieved more quickly by using existing solutions as an initial guess for new calculations.

4. RESULTS

The results are presented in such a way that situations with and without wall solution domains can be compared with each other for the same values of the parameters *Re*, *Pr* and *Gr*. Several realistic values of the ratio, a^*/a, are considered for values of K_r relevant to various typical wall materials and with water as the fluid in the duct. The Reynolds and Grashof numbers of the flow, *Re* and *Gr*, are fixed for all the investigations at 50 and -10000, respectively, and *Pr* is given the value 7.00, so that the fluid can be thought of as being water. The Grashof number is chosen to be large so that in most of the situations considered flow reversals are present in the fluid. The value of $b/(a\,Re)$ is chosen to be 0.5, so that the entry length is long enough for $Z = 0$ to be a good approximation to $Z = -\infty$. The values for N, N^w, NN and N^ξ are chosen to be 40, 20, 200 and 200, respectively. Calculations carried out with $N = 20$, $N^w = 10$, $NN = 100$ and $N^\xi = 100$, suggest that the above grids are sufficiently fine to give an accurate solution, and calculations carried out with $N = 60$, $N^w = 30$, $NN = 300$ and $N^\xi = 300$, suggest that the results presented here for the temperature are correct to within about 6×10^{-4} in the fluid and 3×10^{-4} in the wall, in general, although at $Z = b/(a\,Re)$, $R = 1$ the errors were found to be as large as 3×10^{-2}. However, these errors had little effect on the rest of the solution.

The parameter K_r is chosen to have the values 50, 5 and 0.5, and since the thermal conductivity of water is in the range 0.55–0.68 W m^{-1} K^{-1} [15], this covers wall materials with thermal conductivities in the range 0.275–35.0 W m^{-1} K^{-1}. This range covers pipe materials such as stainless steel, chrome steel and many plastics. Typical values of the ratio a^*/a, for piping in use in common industrial applications lie in the range 1.1–1.4 [16]. Thus a^*/a is chosen to have the values 1.1, 1.25 and 1.4, and nine results are presented, each with a different combination of the parameters K_r and a^*/a, and compared with a result obtained from a model in which the wall solution domain is omitted.

In Figs. 3(a) and (b) contour plots of stream function and non-dimensional temperature are displayed,

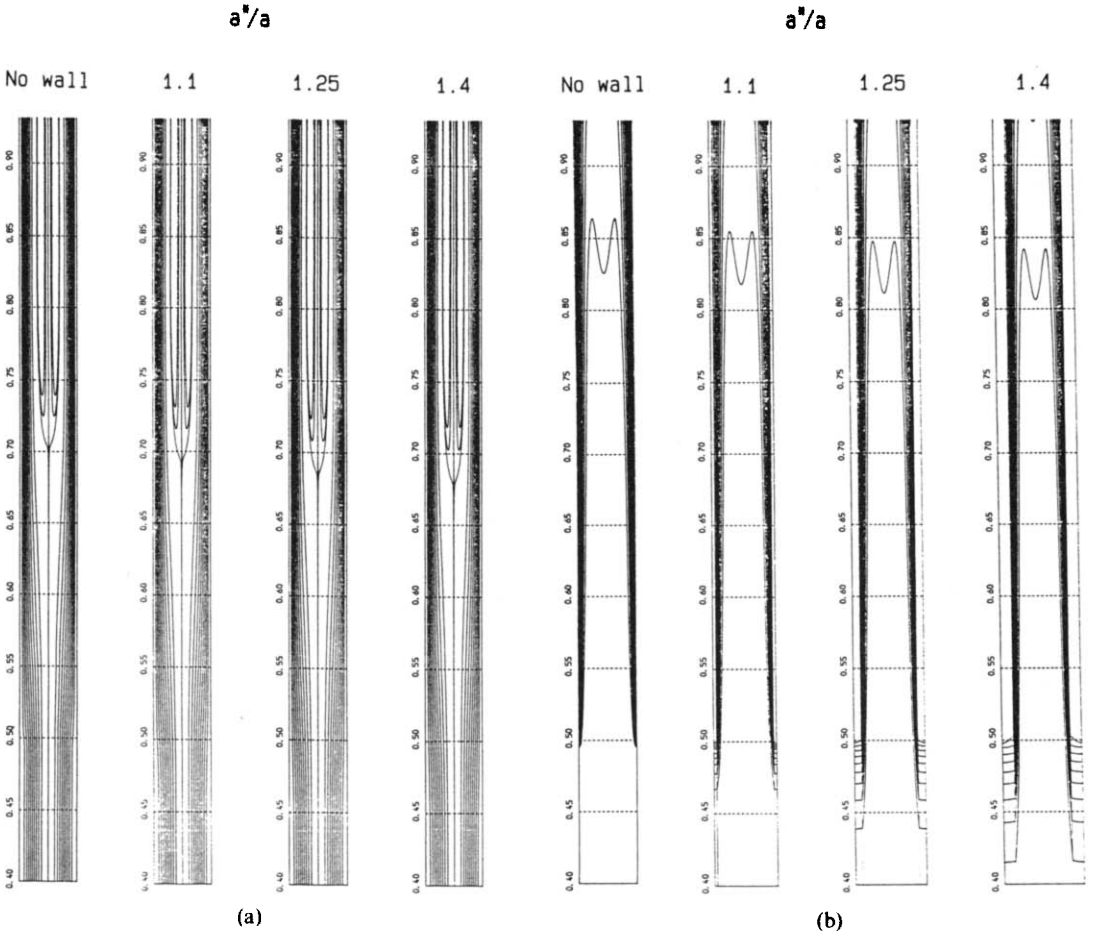

FIG. 3. Contour plots of stream function (a) and temperature (b) for $K_r = 50$, as a^*/a is varied.

respectively, for the case $K_r = 50$. The streamlines plotted are for ψ in the set $\{0.0, 0.05, 0.1, \ldots, 0.4, 0.45, 0.5, 0.501, 0.502\}$, where $\psi = 0.0$ is the streamline along the wall, and the temperature contours are for $\theta_{f,w}$ in the set $\{0.1, 0.2, \ldots, 0.8, 0.9\}$, where $\theta_{f,w} = 0.9$ is the contour nearest to the entrance of the pipe. The first plots are from the investigation with no wall solution domain and they are compared with plots obtained using solutions from the wall problem with $a^*/a = 1.1$, 1.25 and 1.4, respectively. It can be seen from the temperature contours that the effect of the large value of K_r is to conduct the temperature applied for $Z > 0.5$ a significant distance upstream, within the wall. This distance becomes greater as the value of a^*/a increases. This upstream axial conduction in the duct wall causes a significant pre-heating of the water in the tube and this in turn means that the recirculation region at the centre of the pipe begins to form further upstream.

In Figs. 4(a) and (b) K_r is taken to be 5 and contour plots of ψ and $\theta_{f,w}$ are again displayed. For these situations the effects of axial wall conduction are much less significant and, although a certain amount of upstream conduction can be seen to be present in the temperature contours, the effects of convection on the heat transfer process can be seen to have a major effect on the temperature distribution on the inside of the duct wall. In particular, for the case $a^*/a = 1.4$, the temperature contour $\theta_{f,w} = 0.1$ does not pass into the fluid until $Z \gg 0.9$. The beginning of the recirculation region is, as a result, moved further downstream. Comparing Figs. 3 and 4 it seems reasonable to assume that there will be a value of K_r for which the streamlines and temperature contours remain approximately fixed as a^*/a is varied. In Figs. 5(a) and (b) contour plots of ψ and $\theta_{f,w}$ are presented for $K_r = 0.5$ which corresponds to a wall material that is a relatively poor conductor. The penetration of the temperature can be seen to be very restricted from Fig. 5(b) and this causes a more gradual development in the velocity profiles. Reverse flow is present for $a^*/a = 1.1$, the recirculation beginning at around $Z = 0.92$, however, no reverse flow at all is present in the flows for $a^*/a = 1.25$ and 1.4. The wall is in fact acting more like an insulator than a conductor, although a good insulating material would normally have $K_r < 0.05$ for these particular flows.

The flow average temperature, θ_m, local Nusselt number, Nu, and friction factor, f, for the flows under consideration here are defined as follows [14]:

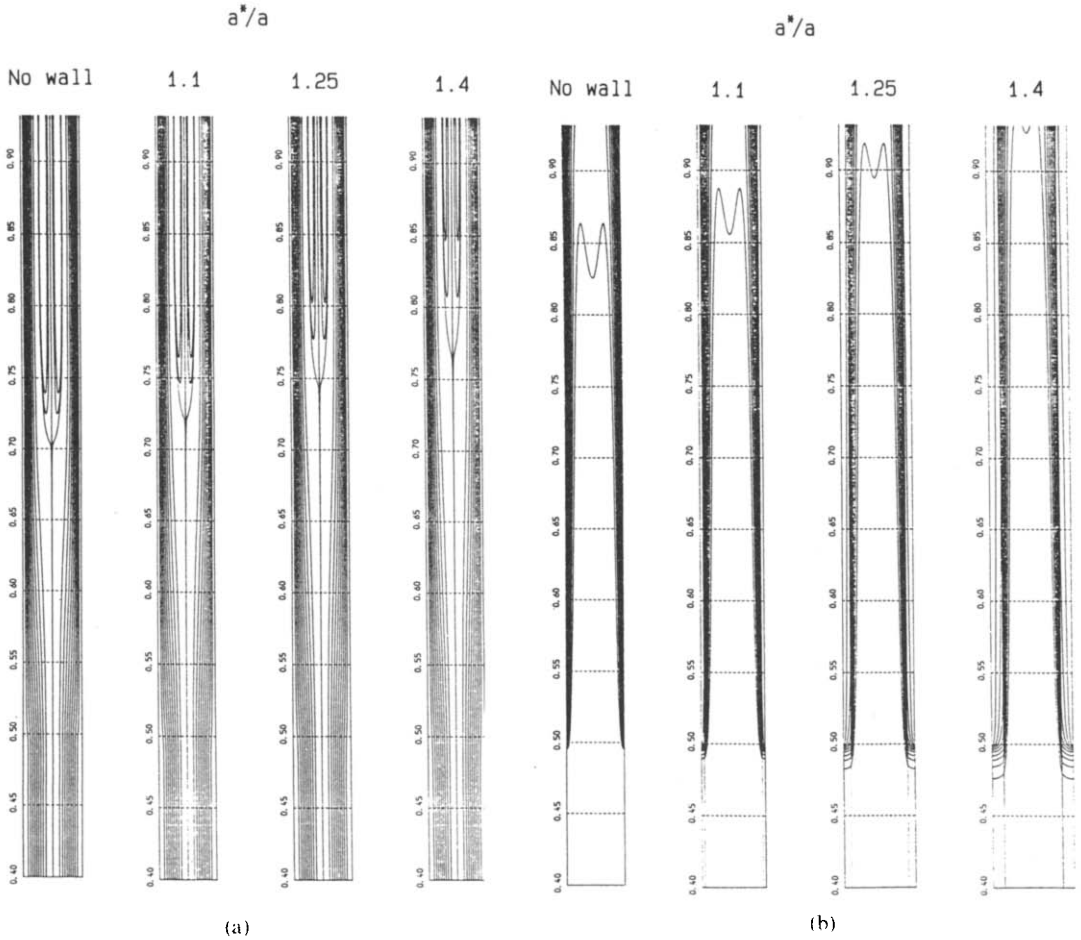

FIG. 4. Contour plots of stream function (a) and temperature (b) for $K_r = 5$, as a^*/a is varied.

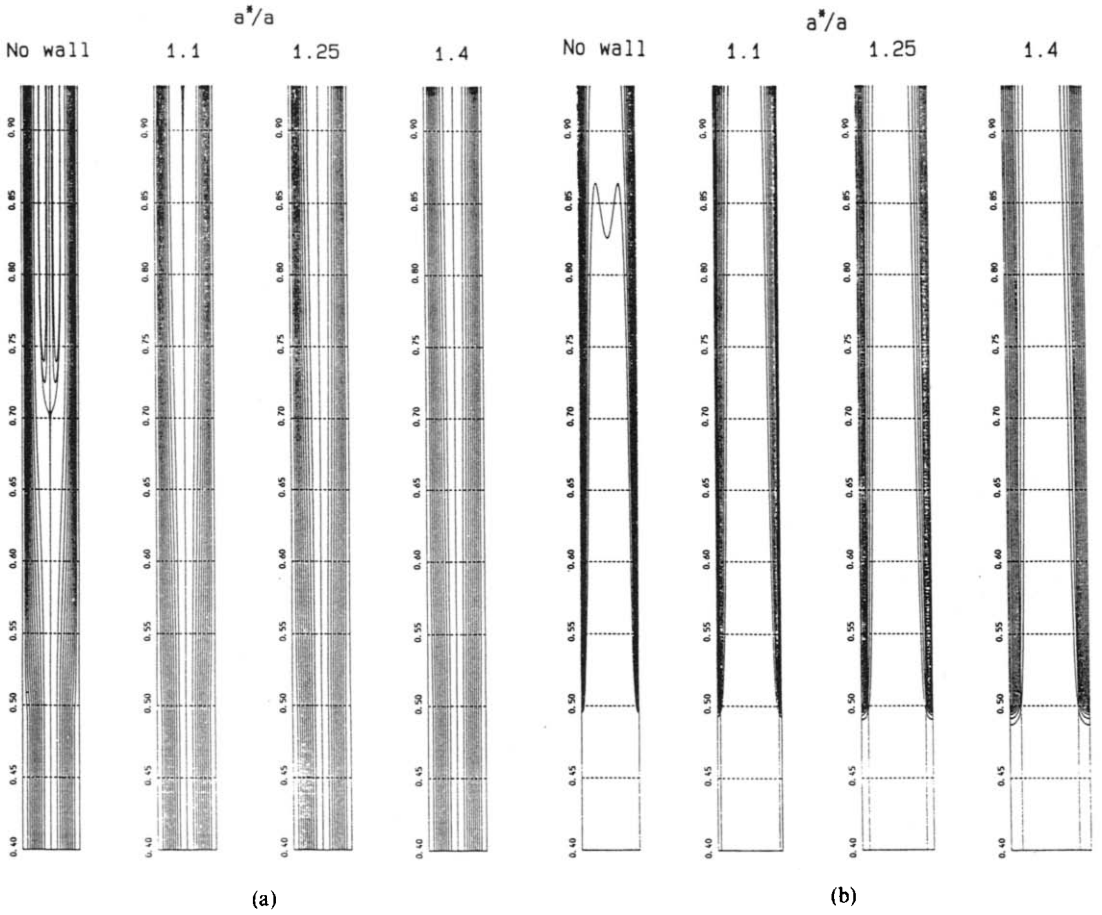

FIG. 5. Contour plots of stream function (a) and temperature (b) for $K_r = 0.5$, as a^*/a is varied.

$$\theta_m = -2\int_0^1 \frac{\partial \psi}{\partial R}\theta_f \, dR \tag{34}$$

$$Nu = -\left.\frac{\partial \theta}{\partial R}\right|_{R=1} \Big/ (\theta_m - \theta|_{R=1}) \tag{35}$$

$$Ref = 8\Omega|_{R=1}. \tag{36}$$

Plots of θ_m, Nu, and Ref, as defined by equations (34)–(36), respectively, are displayed in Figs. 6(a)–(c), respectively, for each of the flows displayed in Fig. 3. The flow average temperature is seen to be affected to a small extent just upstream of $Z = 0.5$, where the sharp drop in θ_m is rounded off as a^*/a increases. However, downstream the plots are almost indistinguishable as θ_m falls away to 0. In Fig. 6(b) the local Nusselt number is seen to take a finite value well upstream of $Z = 0.5$, when the wall solution domain is included in the problem. At first Nu becomes negative because $\theta|_{R=1} > \theta_m$, however, at some point for $Z < 0.5$ the sign of $\theta_m - \theta|_{R=1}$ changes from negative to positive and Nu becomes infinite and changes sign, as can be seen from Fig. 6(b). A further peak is observed in Nu at $Z = 0.5$, where a rapid decrease in $\theta_{f,w}$ at the inside of the wall causes the value of $(\partial\theta_f/\partial R)_{R=1}$ to increase very quickly. Beyond $Z = 0.5$ very little difference in the plots can be observed, as the values decrease towards the usual fully developed value of 1.83 for a flow without a wall solution domain. From Fig. 6(c) the value of Ref is seen to rise earlier from its fully developed value of 32 as a^*/a is increased. This is as would be expected, because the axial conduction in the pipe wall causes the velocity profile in the fluid to start developing upstream of $Z = 0.5$.

In Figs. 7(a)–(c), θ_m, Nu and Ref are displayed, respectively, for the flows described in Fig. 4. The value of θ_m is seen to decrease more slowly as a^*/a is increased in Fig. 7(a). This is as would be expected from the temperature plots in Fig. 4(b). In Fig. 7(b) the behaviour of Nu is similar to that observed in Fig. 6(b), however, the singularities occur much closer to $Z = 0.5$ since the effects of axial wall conduction are much less for these flows. The fully developed values are seen to be slightly lower than the value of 1.83 from the flow without a wall solution domain. The values of Ref in Fig. 7(c) illustrate the slower development of the velocity profile as a^*/a is increased, as would be expected from the streamline plots in Fig. 4.

In Figs. 8(a)–(c), θ_m, Nu and Ref are displayed, respectively, for the flows described in Fig. 5. For each

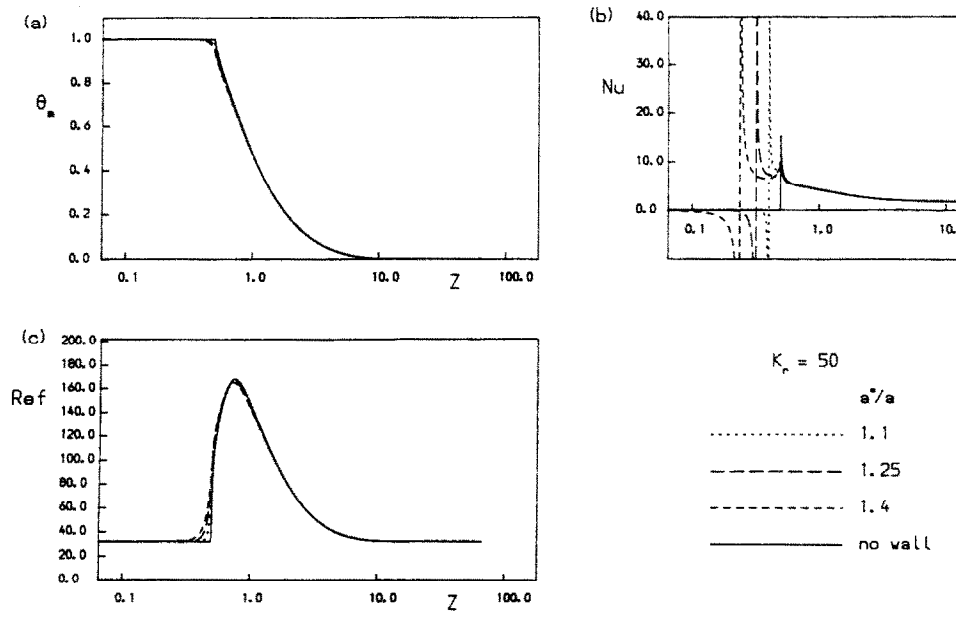

FIG. 6. Plots of flow average temperature, local Nusselt number and friction factor times Reynolds number against axial distance for $K_r = 50$ and the indicated values of a^*/a.

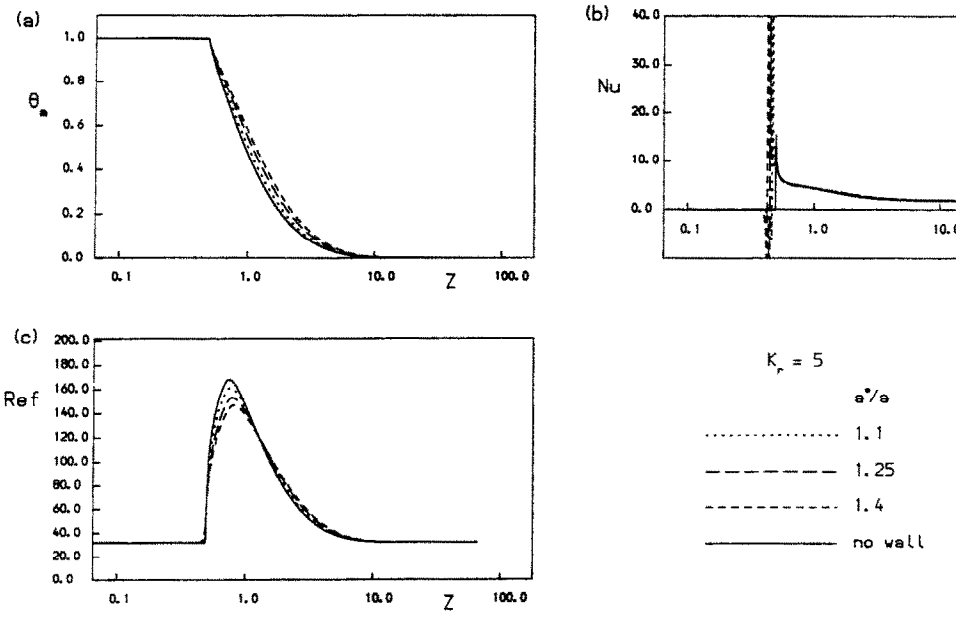

FIG. 7. Plots of flow average temperature, local Nusselt number and friction factor times Reynolds number against axial distance for $K_r = 5$ and the indicated values of a^*/a.

of θ_m, *Nu* and *Ref*, the trends recognized in Fig. 7 are continued to a much greater extent, as the velocity and temperature profiles develop more slowly due to the lower value of K_r.

5. CONCLUSIONS

In this paper, solutions to a combined convection flow in a cylindrical geometry are obtained, when the thermal boundary conditions are applied at the outside of a wall solution domain, inside which the temperature is allowed to vary in both the axial and radial directions. Solutions are obtained for values of the fluid to wall conductivity ratio, K_r, in the range 0.5–50, and for values of the ratio of the outside to the inside radii of the wall, a^*/a, in the range 1.1–1.4. The flows and temperature distributions are seen to be greatly dependent upon the value of K_r, with significant upstream effects being observed for large

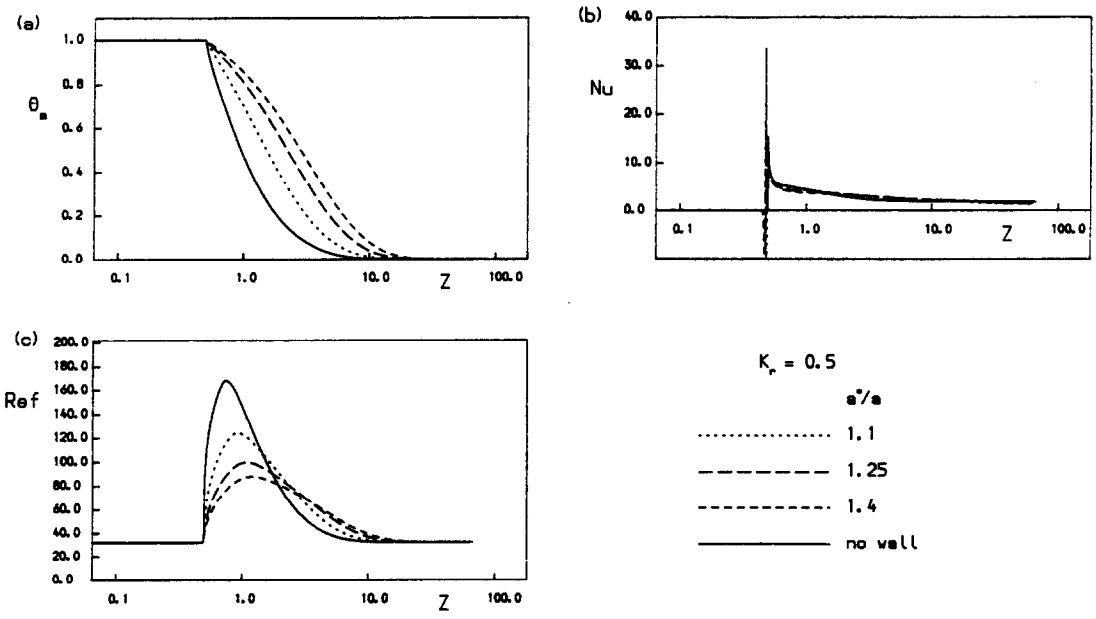

FIG. 8. Plots of flow average temperature, local Nusselt number and friction factor times Reynolds number against axial distance for $K_r = 0.5$ and the indicated values of a^*/a.

values of K_r and significant downstream effects being observed for small values of K_r. These effects were found to be exaggerated for larger values of the ratio a^*/a.

In the recent literature on conjugate heat transfer problems many assumptions are inherent in the mathematical representations and in particular, no account is taken in any of the investigations of the development of the velocity profile within the fluid due to the effects of free convection. In this paper the full elliptic equations, in both the fluid and wall domains, are solved for the first time and results are presented for situations where flow reversals are present. The conclusion to be drawn from this investigation is that in many situations the wall of the flow domain may play a significant part in the characteristics of both the flow and the heat transfer. Careful thought must be taken before discarding the wall domain from the thermal problem, especially with the Reynolds number of the flow is relatively low.

REFERENCES

1. R. K. Shah and A. L. London, Laminar flow forced convection in ducts. In *Advances in Heat Transfer*, Supplement 1. Academic Press, London (1978).
2. G. S. Barozzi and G. Pagliarini, Conjugated heat transfer in a circular duct with uniform and non-uniform wall thickness, *Heat Technol.* **2**, 72–89 (1984).
3. G. S. Barozzi and G. Pagliarini, Experimental investigation of coupled conduction and laminar convection in a circular tube, *Int. J. Heat Mass Transfer* **27**, 2321–2329 (1984).
4. G. S. Barozzi and G. Pagliarini, A method to solve conjugate heat transfer problems: the case of fully developed laminar flow in a pipe, *ASME J. Heat Transfer* **107**, 77–83 (1985).
5. S. Mori, M. Sakakibara and A. Tanimoto, Steady heat transfer to laminar flow in a circular tube with conduction in the tube wall, *Heat Transfer—Jap. Res.* **3**, 37–46 (1974).
6. S. Mori, T. Shinke, M. Sakakibara and A. Tanimoto, Steady heat transfer to laminar flow between parallel plates with conduction in wall, *Heat Transfer—Jap. Res.* **5**, 17–25 (1976).
7. E. K. Zariffeh, H. M. Soliman and A. C. Trupp, The combined effects of wall and fluid axial conduction on laminar heat transfer in circular tubes, *Proc. 7th Int. Heat Transfer Conf.*, Munich, West Germany, Vol. 4, pp. 131–136 (1982).
8. M. Faghri and E. M. Sparrow, Simultaneous wall and fluid axial conduction in laminar pipe-flow heat transfer, *ASME J. Heat Transfer* **102**, 58–63 (1980).
9. A. Campo and R. Rangel, Lumped-system analysis for the simultaneous wall and fluid axial conduction in laminar pipe-flow heat transfer, *PhysioChem. Hydrodyn.* **4**, 163–173 (1983).
10. B. Zeldin and F. W. Schmidt, Developing flow with combined forced-free convection in an isothermal vertical tube, *ASME J. Heat Transfer* **94**, 211–223 (1972).
11. L. C. Chow, S. R. Husain and A. Campo, Effects of free convection and axial conduction on forced convection heat transfer inside a vertical channel at low Peclet number, *ASME J. Heat Transfer* **106**, 297–303 (1984).
12. B. Morton, D. B. Ingham, D. J. Keen and P. J. Heggs, Experimental and numerical investigations into recirculating combined convection in laminar pipe flow, *Proc. Int. Symp. on Natural Circulation*, ASME Winter Annual Meeting, Boston, Massachusetts, December, pp. 331–339 (1987).
13. M. W. Collins, Viscous dissipation effects on developing laminar flow in adiabatic and heated tubes, *Proc. Instn Mech. Engng* **189**, 129–137 (1975).
14. D. J. Keen, Combined convection in heat exchangers, Ph.D. Thesis, University of Leeds, U.K. (1988).
15. M. N. Özişik, *Heat Transfer, a Basic Approach*. McGraw-Hill, New York (1985).
16. F. Kreith, *Principles of Heat Transfer*. Harper & Row, New York (1973).

EFFETS DE LA CONDUCTION THERMIQUE DANS LA PAROI SUR LE DEVELOPPEMENT DES ECOULEMENTS AVEC RETOUR COMBINES DE CONVECTION DANS DES TUBES VERTICAUX

Résumé—On étudie numériquement les effets de la conduction thermique sur un écoulement d'eau laminaire, permanent, mixte et couplé. Les nombres de Prandtl, Reynolds et Grashof sont respectivement fixés à 7,0, 50 et -10000 et le renversement d'écoulement est présent dans la plupart des écoulements considérés. Des essais sont faits en rendant variables le rapport des conductivités paroi fluide et le rapport des rayons extrêmes de la paroi. Des comparaisons avec un écoulement dans lequel on ne considère pas l'influence de la paroi montrent que des changements très sensibles sont obtenus dans l'écoulement et dans les distributions de température quand on prend en compte l'influence de la paroi.

EINFLÜSSE DER WÄRMELEITUNG IN DER WAND EINES SENKRECHTEN ROHRES AUF DIE AUSBILDUNG VON GEMISCHT-KONVEKTIVEN REZIRKULATIONSSTRÖMUNGEN

Zusammenfassung—Der Einfluß der Wärmeleitung in der Wand eines senkrechten Rohres auf die stationäre laminare gemischte Konvektionsströmung von Wasser wird numerisch untersucht. Die Prandtl-, Reynolds- und Grashof-Zahl wird mit 7,0, 50 bzw. -10000 angenommen. In den meisten der betrachteten Fälle tritt eine Rückströmung auf. Die Untersuchungen werden für unterschiedliche Verhältnisse der Wärmeleitfähigkeit von Fluid und Wandmaterial sowie für unterschiedliche Verhältnisse von Außen- und Innendurchmesser durchgeführt. Vergleichende Rechnungen ohne Einbeziehung des Wandbereiches zeigen, daß dessen Berücksichtigung signifikante Änderungen der Strömungs- und Temperaturverteilung hervorruft.

ВЛИЯНИЕ ТЕПЛОПРОВОДНОСТИ СТЕНКИ НА РАЗВИТИЕ ПРОТИВОТОЧНЫХ ТЕЧЕНИЙ В ВЕРТИКАЛЬНЫХ ТРУБАХ ПРИ СМЕШАННОЙ КОНВЕКЦИИ

Аннотация—Численно исследуется влияние теплопроводности стенки при смешанной конвекции на устойчивое ламинарное течение воды в вертикальной трубе. Для потока были выбраны фиксированные значения чисел Прандтля, Рейнольдса и Грасгофа 7,0, 50 и-10000, соответственно, и было найдено, что в большинстве рассматриваемых течений существует противоток. Исследования проведены в диапазонах допустимых изменений отношений коэффициентов теплопроводности стенки и жидкости, а также отношений радиусов внутренней и внешней стенок трубы. Сравнение с течением, для которого не рассматривается решение в пристенной области, показывает, что при учете пристенной области могут наблюдаться очень существенные изменения в распределениях потока и температуры.